

## IEA Wind TCP Task 55: The IEA Wind 740-10-MW Reference Offshore Wind Plants

Kainz, Samuel; Quick, Julian; Souza de Alencar, Mauricio; Sanchez Perez Moreno, S.; Dykes, Katherine ; Bay, Christopher; Zaaier, M B; Bortolotti, Pietro

**DOI**

[10.2172/2333634](https://doi.org/10.2172/2333634)

**Publication date**

2024

**Document Version**

Final published version

**Citation (APA)**

Kainz, S., Quick, J., Souza de Alencar, M., Sanchez Perez Moreno, S., Dykes, K., Bay, C., Zaaier, M. B., & Bortolotti, P. (2024). *IEA Wind TCP Task 55: The IEA Wind 740-10-MW Reference Offshore Wind Plants*. National Renewable Energy Laboratory NREL. <https://doi.org/10.2172/2333634>

**Important note**

To cite this publication, please use the final published version (if applicable).  
Please check the document version above.

**Copyright**

Other than for strictly personal use, it is not permitted to download, forward or distribute the text or part of it, without the consent of the author(s) and/or copyright holder(s), unless the work is under an open content license such as Creative Commons.

**Takedown policy**

Please contact us and provide details if you believe this document breaches copyrights.  
We will remove access to the work immediately and investigate your claim.

March 2024

**IEA Wind TCP Task 55**

**The IEA Wind  
740-10-MW Reference  
Offshore Wind Plants**



**iea wind**

**Prepared for the  
IEA Wind TCP**



**March 2024**

**Authors:**

Samuel Kainz  
Wind Energy Institute, Technical University of Munich

Julian Quick  
Department of Wind and Energy Systems, Technical University of Denmark

Mauricio Souza de Alencar  
Department of Wind and Energy Systems, Technical University of Denmark

Sebastian Sanchez Perez Moreno  
Wind Energy Section, Delft University of Technology

Katherine Dykes  
Department of Wind and Energy Systems, Technical University of Denmark

Christopher Bay  
National Renewable Energy Laboratory

Michiel B. Zaaijer  
Wind Energy Section, Delft University of Technology

Pietro Bortolotti  
National Renewable Energy Laboratory

*IEA Wind TCP functions within a framework created by the International Energy Agency (IEA). Views, findings, and publications of IEA Wind do not necessarily represent the views or policies of the IEA Secretariat or of all its individual member countries. IEA Wind is part of IEA's Technology Collaboration Programme (TCP).*

## Abstract

This report describes the first version of the regular and irregular IEA Wind 740-10-MW Reference Offshore Wind Plants (v0.1). The two plants have been developed within the second work package of the International Energy Agency Wind Technology Collaboration Programme (IEA Wind) Task 37 on Wind Energy Systems Engineering: Integrated Research, Development, and Demonstration. The plants aim to act as reference for future research projects on wind energy, representing modern offshore wind plants. The designs are based on the Borssele III and IV offshore wind plant projects. The associated wind resource, allotted territory, and bathymetry measurements are used to define the site characteristics. Seventy-four IEA 10-MW Reference Wind Turbines are arranged in two suggested layouts that are optimized for maximum annual energy production: one regular grid layout and one irregular layout. For both layouts, collection system networks with minimized total cabling length are defined. The reference wind plants have been described using the WindIO ontology and have been made available through the open-source repository <https://github.com/IEAWindTask37/IEA-Wind-740-10-ROWP>.

# Contents

<b>1</b>	<b>Introduction</b>	<b>3</b>
<b>2</b>	<b>Definition of the IEA Wind 740-10-MW Reference Offshore Wind Plants (v0.1)</b>	<b>5</b>
2.1	Reference site . . . . .	5
2.2	Reference turbine . . . . .	7
2.3	Reference layouts . . . . .	8
2.4	Reference collection networks . . . . .	9
<b>3</b>	<b>Next Steps</b>	<b>11</b>
<b>A</b>	<b>Regular Layout</b>	<b>15</b>
<b>B</b>	<b>Irregular Layout</b>	<b>16</b>

## List of Tables

1	Vertices defining the boundaries of the reference wind plant zone, and location of the offshore substation. . . . .	5
2	Sectoral Weibull distributions and corresponding relative frequencies of the wind resource for 30° bins at hub height. . . . .	6
3	Main characteristics of the IEA 10-MW Reference Wind Turbine. . . . .	7
4	Cabling types used for the IEA Wind 740-10-MW ROWPs. . . . .	10
5	Turbine coordinates and power cable connections for the regular grid layout. . . . .	15
6	Turbine coordinates and power cable connections for the irregular layout. . . . .	16

## List of Figures

1	Visualization of the real Borssele III and IV wind plants, the surrounding Belgian–Dutch offshore wind plant cluster, and the merged wind plant zone, based on OpenStreetMap data. . . . .	4
2	Trends in relative frequencies per wind direction bin for different heights, and interpolation results at hub height. . . . .	5
3	Wind rose of the Borssele site at hub height. . . . .	6
4	(a) Electric power and thrust curves, and (b) aerodynamic power coefficients ( $C_p$ ) and thrust coefficients ( $C_t$ ) of the IEA 10-MW Reference Wind Turbine. . . . .	7
5	The layouts defined in the reference site. . . . .	8
6	Normalized power production corresponding to the regular and irregular ROWPs as computed with PyWake. . . . .	9

# 1 Introduction

Standard reference cases allow for an unambiguous comparison of different multidisciplinary design, analysis, and optimization tools. Over the years, the reference wind turbines developed within the International Energy Agency Wind Technology Collaboration Programme (IEA Wind) have become valuable tools for the research and business communities. In contrast to reference turbines, which are widely used and accepted, there are no established reference plants, either offshore or land-based. In fact, reference turbines placed in simple geometric layouts and real wind plants with accessible data have mainly served as case studies for wind plant analysis so far. For the latter case, well-known examples are Alpha Ventus [1], Anholt, and Westermøst Røst [2]. However, simple geometric layouts do not address the complexity of wind plant design and control as a whole and are therefore typically restricted to specific applications, e.g., when comparing different wake steering strategies. On the other hand, data access for real wind plants is typically limited, and critical information such as the aeroelastic design of turbine components or the control trajectory are not accessible. Therefore, comparison of studies focusing on the same wind plant is hindered in general.

So far, there have been three notable academic efforts to introduce reference offshore wind plants: the NOWITECH, the NORCOWE, and the Total Control wind plants. The NOWITECH Reference Wind Farm consists of 120 adapted Technical University of Denmark (DTU) 10-MW reference machines evenly spaced in three clusters and features a high-voltage direct current (HVDC) connection to shore [3]. For the NORCOWE reference plant, 80 DTU 10-MW machines have been arranged in a perimeter-weighted curvilinear layout and a regular variant; both cases feature a high-voltage alternating current (HVAC) connection to shore [4]. The Total Control Reference Wind Power Plant comprises 32 IEA 10-MW reference machines placed in a staggered regular pattern [5] and has been developed to investigate control strategies. Additional relevant references are the IEA Wind Task 37 case studies 3 and 4 [6], located at the same site as the plants described in this report. Based on Case Study 4, a recent publication [7] compared performance of eight different wind plant layout optimization algorithms considering exclusive zones.

However, the mentioned reference plants are limited in data definition and provision, which complicates their ability to function as commonly accepted reference cases for varying application purposes. For instance, turbine coordinates or bathymetry are not provided for the NORCOWE and the NOWITECH reference plants, and the Total Control Reference Wind Power Plant is not located at a specific site. Furthermore, none of these plants comes with an open-source repository that gives access to the underlying data.

In an effort to provide holistically defined and broadly applicable reference plants, the IEA Wind Task 37 team has decided to develop several IEA Wind reference wind plants. These plants shall provide extensive and easily accessible information on site characteristics, plant design, and turbine definition, allowing for diversified and comprehensive studies with varying analysis and optimization objectives. IEA Wind Task 37 has worked out the first version of the first two reference plants in this series: the regular and irregular IEA Wind 740-10-MW Reference Offshore Wind Plants (ROWPs), which are introduced in this paper. IEA Wind Task 55, which builds on Task 37 and is dedicated to defining land-based and offshore reference plants and turbines, will further develop the IEA Wind 740-10-MW ROWPs and introduce new reference wind plants, both land-based and offshore [8].

The IEA Wind 740-10-MW ROWPs (v0.1) are based on two real wind plants, the Borssele Offshore Wind Farms III and IV, that are merged into a single wind plant zone. Borssele III and IV are part of the Belgian–Dutch offshore wind plant cluster and are surrounded by several other wind plants, visualized in Figure 1. Combined, the two wind plants consist of 77 Vestas

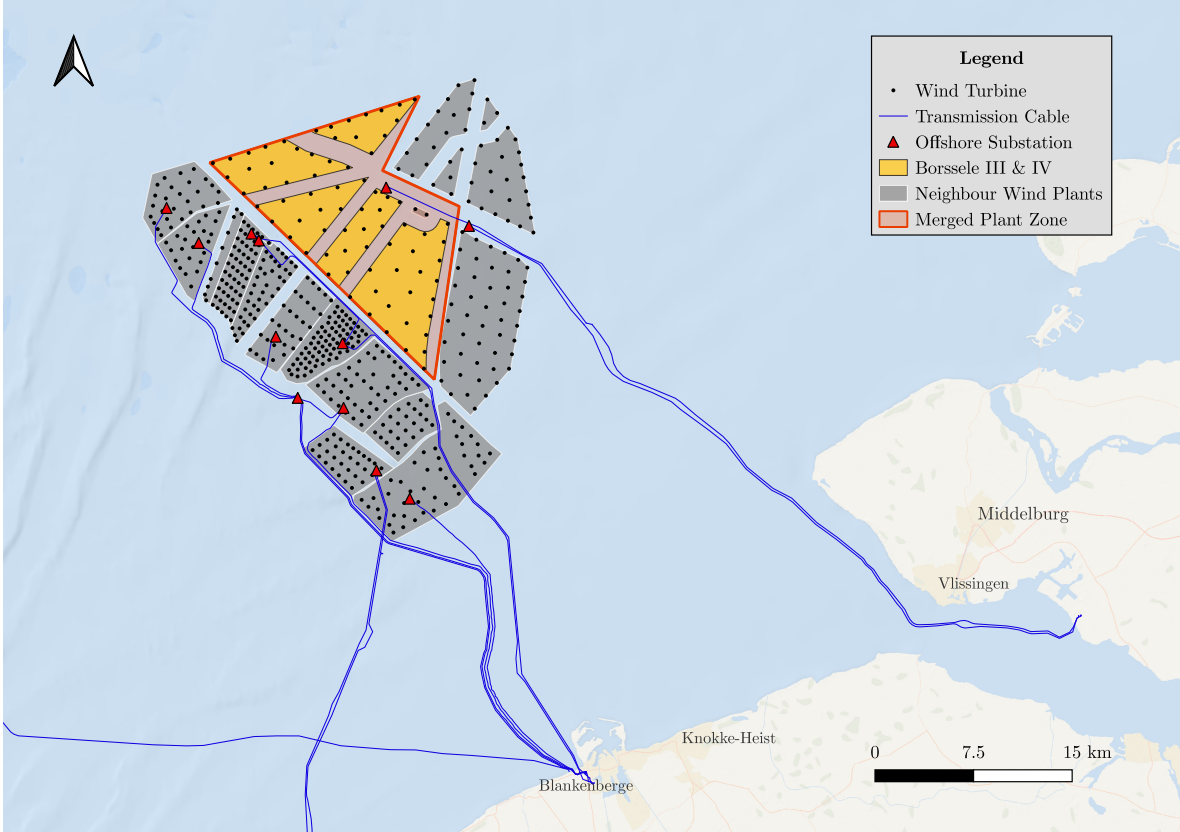


Figure 1: Visualization of the real Borssele III & IV wind plants, the surrounding Belgian–Dutch offshore wind plant cluster, and the merged wind plant zone, based on OpenStreetMap data [11].

V164-9.5 turbines, resulting in a total capacity of 731.5 MW. To ensure similar turbine power and plant capacity, the IEA Wind 740-10-MW ROWPs (v0.1) have been populated with 74 IEA 10-MW reference turbines, resulting in a plant capacity of 740 MW. The presented reference plants are named after the total plant capacity and the rated power of the selected reference turbines. Two layouts that are optimized for annual energy production (AEP) are introduced in this paper: a regular grid layout resulting from foregoing work [9], and an irregular layout optimized using the TOPFARM stochastic gradient descent optimization implementation [10]. This is the first version of the IEA Wind 740-10-MW ROWPs; further relevant definitions such as support structure dimensions will be provided in a future version of the plants.

For improved interoperability and fostered collaboration, the IEA Wind Task 37 team has developed a classification system and ontology allowing for common representation of data: WindIO [12, 13]. The WindIO framework has been successfully applied to define many reference wind turbines. Similarly, WindIO allows for standardized representation of wind plant data. Therefore, the IEA Wind 740-10-MW ROWPs (v0.1) are released following the standards of WindIO. The data are published in a public repository [14].

## 2 Definition of the IEA Wind 740-10-MW Reference Offshore Wind Plants (v0.1)

### 2.1 Reference site

The Dutch government has made metocean data on the Borssele site publicly available [15], which is beneficial for the design of reference plants with correlated and consistent wind, ocean, and bathymetry data. It was decided to combine regions III and IV to match a wind plant nominal rating of 740 MW. These two regions were joined into a simply connected space. The boundaries of the zone are defined as a polygon with vertices given in Table 1. The table also lists the coordinates of the offshore substation [16], located on the northeast side of the boundaries between sites III and IV, and roughly 40 km from the shore.

The characterization of the wind resource is based on the official resource report for Borssele III [17]. Shear is characterized through a power-law profile with  $\alpha = 0.08$ . This profile is used to scale the sectoral Weibull distributions as provided in ref. [17] from 100 m to hub height (119 m). Veer is not included in the resource definition of the ROWPs, but was considered when interpolating

Table 1: Vertices defining the boundaries of the reference wind plant zone, and location of the offshore substation (S). Coordinates refer to the EPSG:25831 coordinate reference system.

Coordinates		
#	Northing [m]	Easting [m]
1	484,178.6	5,732,482.8
2	500,129.9	5,737,534.4
3	497,318.1	5,731,880.2
5	503,163.4	5,729,155.3
6	501,266.5	5,715,990.1
7	488,951.0	5,727,940.0
S	497,620.7	5,730,622.0

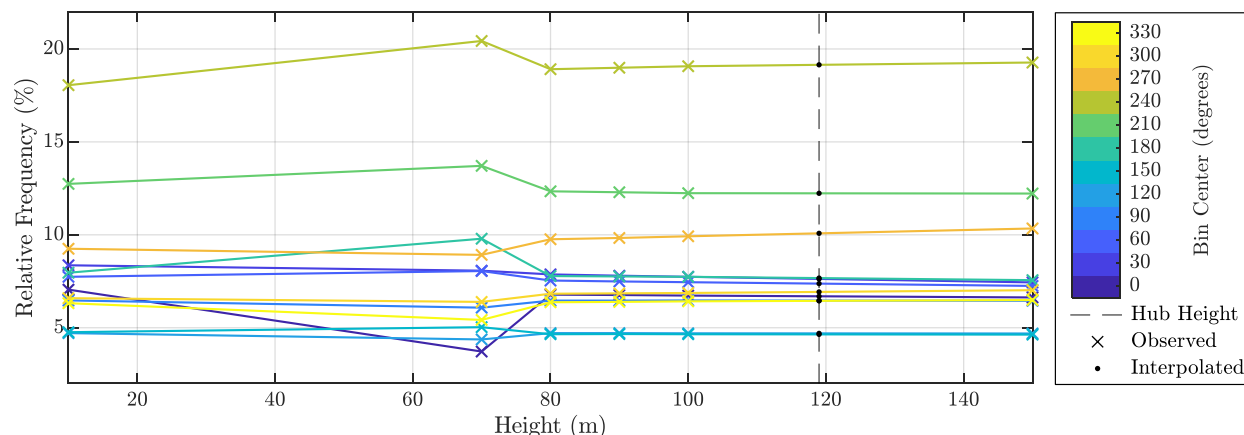


Figure 2: Trends in relative frequencies per wind direction bin for different heights based on data from the annex of ref. [17], and interpolation results at hub height. The different lines refer to the relative frequencies in  $30^\circ$  sector bins with bin centers as indicated in the legend.



Table 2: Sectoral Weibull distributions and corresponding relative frequencies of the wind resource for 30° bins at hub height.

Bin center [degrees]	Scale [m/s]	Shape [-]	Rel. frequency [%]
0	9.08	2.22	6.69
30	9.30	2.26	7.63
60	9.18	2.28	7.37
90	8.89	2.28	6.46
120	8.13	2.15	4.70
150	8.76	2.11	4.64
180	11.38	2.13	7.67
210	12.58	2.29	12.23
240	12.74	2.43	19.15
270	10.80	2.09	10.08
300	9.76	2.01	6.93
330	9.63	2.01	6.45

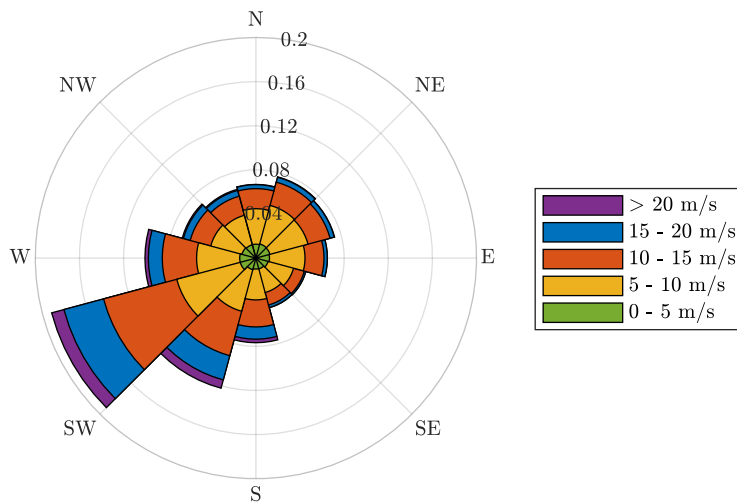


Figure 3: Wind rose of the Borssele site at hub height. The radial axis indicates the cumulative relative frequency of occurrence of wind speeds per sector.

the frequency data available at six different heights to hub height. The relative frequencies per wind direction bin scale approximately linearly with height from about 80 m on, as visualized in Figure 2, and are therefore linearly interpolated to hub height using data at heights of 100 m and 150 m. The resulting scaled sectoral Weibull distributions and relative frequencies per wind direction bin at hub height are provided in Table 2. The wind resource is dominated by inflow from southwestern directions, as visualized in Figure 3.

Turbulence is specified as a function of the 10-min average wind speed, approximated with data from the offshore research platform “FINO1” (as part of the “Research in North and Baltic Sea” project [18]) as suggested by ref. [17]. For heights greater than 70 m, the following empirical

relation between standard deviation,  $\sigma_{U_h}$ , and 10-min average wind speed,  $U_h$ , holds:

$$\sigma_{U_h} = 0.03U_h + 0.455 \text{ m/s} \quad (1)$$

In terms of turbulence intensity (TI), this relationship is equivalently:

$$TI = \frac{\sigma_{U_h}}{U_h} = 0.03 + \frac{0.455 \text{ m/s}}{U_h} \quad (2)$$

The site bathymetry was graphically extracted from ref. [17], and the data are provided in the plants repository [14].

## 2.2 Reference turbine

The IEA Wind 740-10-MW ROWPs (v0.1) are populated with 74 IEA 10-MW reference turbines, described in detail in ref. [19]. The main turbine characteristics are presented in Table 3. The turbine performance was computed with CCBlade [20] and is available in the official reference turbine repository [21]. CCBlade is a blade element momentum method for analyzing wind turbine aerodynamic performance. Aeroelastic aspects are not taken into account. A constant generator efficiency of 94.4% [19] was assumed to calculate the electric power output of the turbines. Electric power, thrust, aerodynamic power coefficients, and thrust coefficients are plotted in Figure 4. Electric power curve and thrust coefficients are used to define the turbine performance in the reference plant repository [14].

Table 3: Main characteristics of the IEA 10-MW Reference Wind Turbine [19].

Parameter	Value	Unit
Rated power	10	MW
Rotor diameter	198	m
Hub height	119	m
Cut-in wind speed	4	m/s
Cut-out wind speed	25	m/s
Generator efficiency	94.4	%

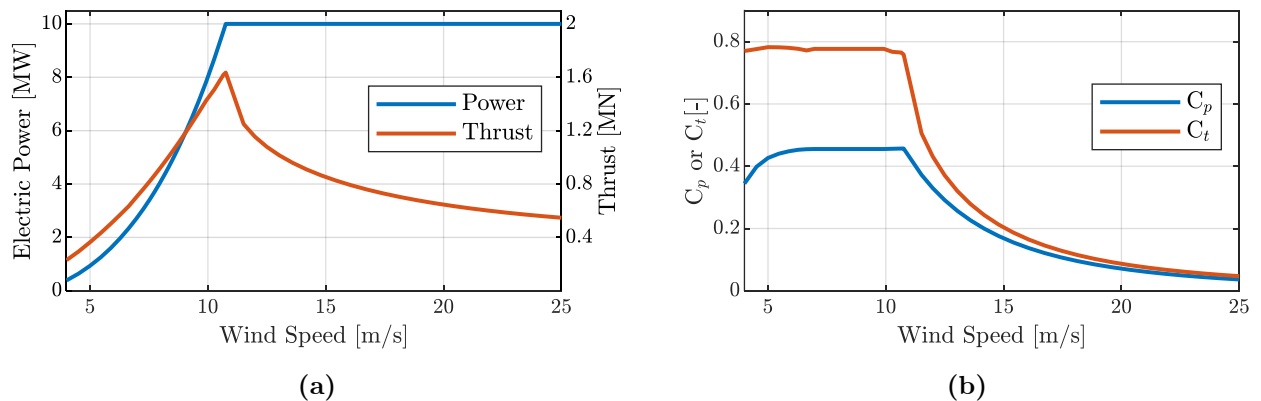


Figure 4: (a) Electric power and thrust curves, and (b) aerodynamic power coefficients ( $C_p$ ) and thrust coefficients ( $C_t$ ) of the IEA 10-MW Reference Wind Turbine [21].

### 2.3 Reference layouts

The optimization objective for this first version of the IEA Wind 740-10-MW ROWPs is optimizing layouts for maximized AEP. The resulting layouts, bathymetry, boundaries, and cable connections are visualized in Figure 5. The site is defined either with a regular grid or irregular layout. The regular layout is the sequentially optimized grid layout described by Perez-Moreno *et al.* [9], where the spacing between turbines is constant. The irregular layout is the result of an AEP optimization using the TOPFARM stochastic gradient descent optimization implementation [10]. The optimizer was run using 10,000 optimization iterations, an initial learning rate of one rotor diameter, and an early stopping threshold of 5%. Turbine spacing was constrained with a minimum distance of two rotor diameters. AEP evaluations were performed using PyWake version 2.5.0 [22]. Wake effects were sampled for wind conditions at a grid with a step size of 1 m/s and  $1^\circ$  for wind speed and direction, respectively. The according probability mass was linearly interpolated based on the data provided in Table 2 using PyWake. The Jensen wake model [23, 24] with a decay coefficient of 0.05 as suggested by ref. [25] was applied to calculate velocity deficits, which were combined using root-sum-square superposition [22]. No rotor averaging model was applied; the wind speed at rotor center point was considered to be representative for the wind speed over the entire rotor. Only intra-farm wake effects were considered in the AEP evaluation, other losses (such as wake effects of the surrounding wind plants, electrical losses in cables and substation, or downtime due to maintenance or curtailment) were not taken into account.

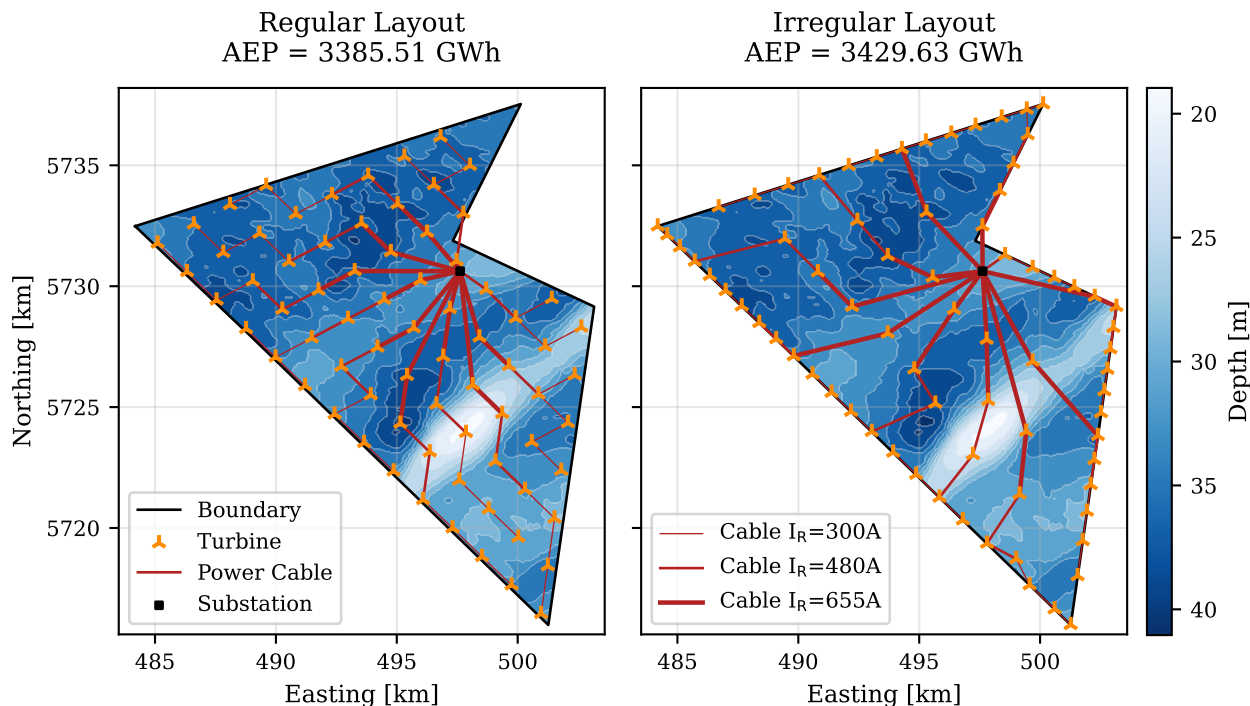


Figure 5: The regular grid (left) and irregular (right) layouts defined in the reference site. Coordinates refer to the EPSG:25831 coordinate reference system. The turbine locations are shown with orange markers. The local bathymetry is visualized as a filled contour plot, within the boundaries of the wind plant, where darker colors indicate greater depths. Cable connections are shown as red lines; a thicker line width indicates cable types with higher current-carrying capacity. The properties of the three applied cables are provided in Table 4.

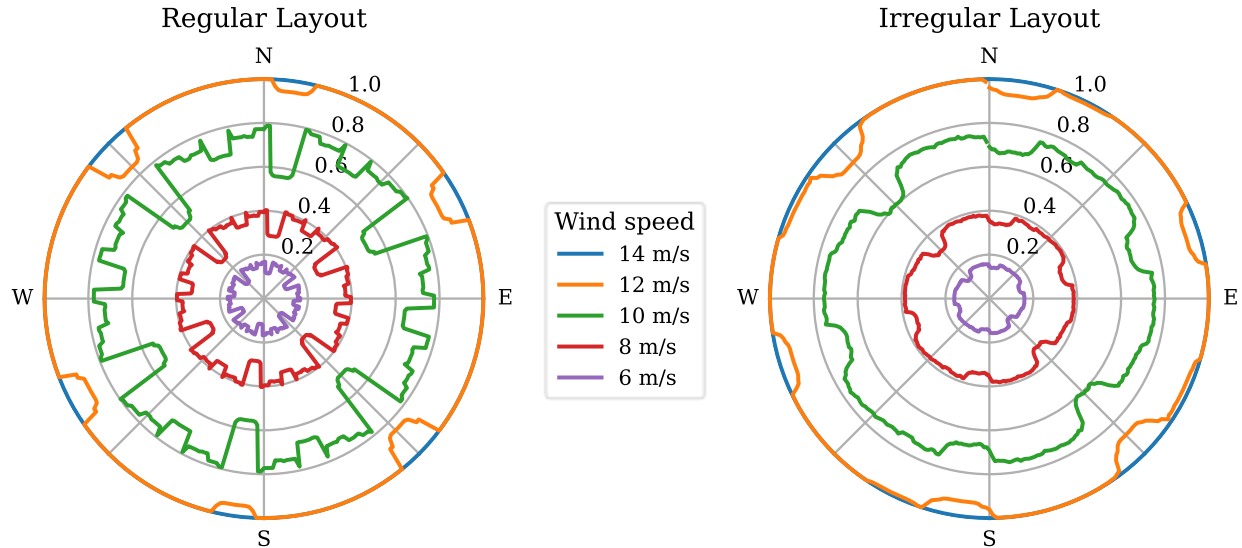


Figure 6: Normalized power production corresponding to the regular and irregular ROWPs as computed with PyWake. The angular axis depicts the wind direction. On the radial axis, plant power normalized by plant capacity (740 MW) is plotted for five different wind speeds.

Figure 6 presents the power production of the two ROWPs normalized by plant capacity (740 MW) for five different wind speeds computed with PyWake as described previously. The calculated AEP of the plant with regular grid layout (3,385.5 GWh) is 1.3 % lower than for the one with irregular layout (3,429.6 GWh) due to higher wake losses at certain inflow directions.

The optimized turbine coordinates for the regular grid layout and the irregular layout are listed in Appendix A and B, respectively. The complete data defining the IEA Wind 740-10-MW ROWPs (v0.1) is provided in an official repository [14] following the WindIO schema. Additionally, the repository includes example files to evaluate the optimized wind plant layouts for AEP using FLORIS [26] and PyWake [22], and the TOPFARM [27] script used to generate the irregular layout.

## 2.4 Reference collection networks

The electrical networks were designed respecting the current-carrying capacity of the cable types presented in Table 4. By setting the collection system voltage level at  $U_R = 66$  kV and given the turbine's rated power  $P_R = 10$  MW, the turbine's rated current  $I_R$  is obtained:

$$I_R = \frac{P_R}{\sqrt{3}U_R} \quad (3)$$

From  $I_R$  and the current capacity of each cable type, the maximum number of turbines that can be served by each cable type is calculated, considering nominal power production and neglecting the reactive power introduced by the cables themselves. This simplifies the optimization problem, as it decouples cable capacity from cable length. After obtaining an optimal layout, the adequacy of the cable types assigned can be ensured by verifying that the vector sum of real and reactive current phasors does not exceed the cable current capacity at any production state. The real current corresponds to the active power being transferred, while the reactive current is the required

Table 4: Cabling types used for the IEA Wind 740-10-MW ROWPs [28].

Parameter	Unit	Cable Nr.		
		1	2	3
Cross section	mm <sup>2</sup>	95	240	500
Current Capacity	A	300	480	655
Max. turbines supplied	-	3	5	7
Charging current per phase at 50 Hz	A	2.0	2.6	3.5
Max. length considering charging current	km	72.7	76.0	66.4

charging current for a given cable length and voltage. The limits for cable length considering the current capacity in excess of the rated turbine currents is shown in Table 4. As long as each connection distance obtained in the optimization is below those limits, the cable currents are within the specification, which is the case for the layouts presented in this report. It is assumed that the wind turbines at the ends of each cable segment will provide the required charging currents, since these are, in all connections, just a fraction of a turbine’s  $I_R$ . A more thorough evaluation could take into account the reactive power capability of the generators which is, however, not specified for the reference turbines used here.

The routing of the cables given the positions of turbines and substation was approached as a Capacitated Minimum Spanning Tree problem, where the capacity (in terms of turbine units served) is defined by the cable type that can carry the highest current. As additional constraints, crossings of cables is prohibited and cable branching is only allowed in a turbine location. The collection system networks shown in Figure 5 were obtained through solving an integer programming model of the problem, which minimizes total cable length. The model was generated by DTU’s EDWIN [29] and the optimal solution was produced by the MILP solver Coin-OR Branch-and-Cut (CBC) [30], called from within EDWIN. Both packages are open-source software and the Python script to generate the layouts can be found in ref. [31]. After obtaining the optimized connections, EDWIN was used to assign the cable types by choosing the lowest capacity cable type that is required for each segment. The results are provided in Appendix A and B as well as in the online repository.

### 3 Next Steps

This report documented the initial development of the first two plants in a series of IEA Wind reference wind plants. These two plants have been developed through the IEA Wind Task 37 team. As the work continues with Task 55, we plan to release several reference wind plants, both land-based and offshore. We also plan to extend the WindIO ontology to allow for richer expressions of the wind resource and the associated turbine responses.

These preliminary layouts were optimized for AEP, which does not take the bathymetry field into account. In future work, we plan to extend the optimization to take bathymetry into account, to consider costs and value in the optimization objective, and to include effects of neighbour wind plants on the flow field. Afterwards, we will release an updated version of the IEA Wind 740-10-MW Reference Offshore Wind Plants.

## Acknowledgments

The development of the IEA Wind 740-10-MW ROWPs has benefited from all activities related to IEA Wind Task 37, and the authors would like to thank all partners involved in the project for their efforts. This work has been partially supported by the MERIDIONAL and the FLOW projects, which receive funding from the European Union's Horizon Europe Programme under the grant agreement No. 101084216 and 101084205, respectively. Sebastian Sanchez Perez-Moreno's work was financed by the Mexican National Council for Science and Technology (CONACYT).

This work was authored in part by the National Renewable Energy Laboratory, operated by Alliance for Sustainable Energy, LLC, for the U.S. Department of Energy (DOE) under Contract No. DE-AC36-08GO28308. Funding provided by U.S. Department of Energy Office of Energy Efficiency and Renewable Energy Wind Energy Technologies Office. The views expressed in the article do not necessarily represent the views of the DOE or the U.S. Government. The U.S. Government retains and the publisher, by accepting the article for publication, acknowledges that the U.S. Government retains a nonexclusive, paid-up, irrevocable, worldwide license to publish or reproduce the published form of this work, or allow others to do so, for U.S. Government purposes.

## References

- [1] Fraunhofer Institute for Wind Energy Systems. *RAVE: Research at alpha ventus*. <https://rave-offshore.de/en/start.html>. Accessed: 2023-09-25.
- [2] Ørsted. *Offshore Wind Measurement & Operational Data*. <https://orsted.com/en/what-we-do/renewable-energy-solutions/offshore-wind/offshore-wind-data>. Accessed: 2023-09-25.
- [3] Henrik Kirkeby and John Olav Tande. “The NOWITECH Reference Wind Farm.” In: *Energy Procedia* 53 (2014), pp. 300–312.
- [4] Thomas Bak et al. “Baseline layout and design of a 0.8 GW reference wind farm in the North Sea.” In: *Wind Energy* 20.9 (2017), pp. 1665–1683.
- [5] Søren Andersen et al. *TotalControl Reference Wind Power Plant: D1.03*. Total Control Deliverable. 2018.
- [6] Nicholas F. Baker et al. *Wind Farm Layout Optimization Case Studies 3 & 4*. IEA Task 37 on System Engineering in Wind Energy announcement. 2019.
- [7] Jared J. Thomas et al. “A comparison of eight optimization methods applied to a wind farm layout optimization problem.” In: *Wind Energy Science* 8.5 (2023), pp. 865–891.
- [8] The International Energy Agency. *IEA Wind TCP Task 55*. <https://iea-wind.org/about-iea-wind-tcp/about-iea/>. Accessed: 2023-10-09.
- [9] S Sanchez Perez-Moreno et al. “Multidisciplinary design analysis and optimisation of a reference offshore wind plant.” In: *Journal of Physics: Conference Series*. Vol. 1037. IOP Publishing. 2018.
- [10] Julian Quick et al. “Stochastic gradient descent for wind farm optimization.” In: *Wind Energy Science* 8 (2023), pp. 1235–1250.
- [11] OpenStreetMap contributors. *Planet dump retrieved from https://planet.osm.org*. <https://www.openstreetmap.org>. 2017.
- [12] Pietro Bortolotti, Evan Gaertner, and Katherine Dykes. *System modeling frameworks for wind turbines and plants*. Tech. rep. NREL, 2020.
- [13] Pietro Bortolotti et al. *System Modeling Frameworks for Wind Turbines and Plants: Review and Requirements Specifications*. Tech. rep. NREL, 2022.
- [14] IEA Wind Task 37. *IEA-Wind-740-10-ROWP*. <https://github.com/IEAWindTask37/IEA-Wind-740-10-ROWP>. Accessed: 2024-02-22.
- [15] The Netherlands Enterprise Agency. *Borssele-Studies*. Available under <https://offshorewind.rvo.nl/cms/view/78f1a154-5b56-4ab0-a70f-d746a610179e/studies-borssele>, Accessed: 2023-09-18.
- [16] R. van der Heijden. *Borssele Wind Farm Zone, Wind Farm Sites I-V, Appendix C: Boundaries and coordinates*. The Netherlands Enterprise Agency. 2017. Available under <https://offshorewind.rvo.nl/cms/view/78f1a154-5b56-4ab0-a70f-d746a610179e/studies-borssele>, Accessed: 2023-09-12.
- [17] H. J. Riezebos, R. de Graaff, and J. Schouten. *Site Studies Wind Farm Zone Borssele: Meteorological study for the Borssele Wind Farm Zone Site III*. The Netherlands Enterprise Agency. 2015. Available under <https://offshorewind.rvo.nl/cms/view/4a3ea5ce-d027-4483-b471-00e5ed87a3bb/studies-borssele-iii-iv-v>, Accessed: 2023-09-12.



- [18] Forschungs- und Entwicklungszentrum Fachhochschule Kiel GmbH. *FINO1 - Research Platform in the North and Baltic Seas No. 1*. <https://www.fino1.de/en/>. Accessed: 2023-08-22.
- [19] Pietro Bortolotti et al. *IEA Wind Task 37 on Systems Engineering in Wind Energy – WP2.1 Reference Wind Turbines*. Tech. rep. International Energy Agency, 2019. URL: <https://www.nrel.gov/docs/fy19osti/73492.pdf>.
- [20] National Renewable Energy Laboratory. *CCBlade*. <https://github.com/WISDEM/CCBlade>. Accessed: 2023-08-30.
- [21] IEA Wind Task 37. *IEA-10.0-198-RWT*. <https://github.com/IEAWindTask37/IEA-10.0-198-RWT>. Accessed: 2023-08-30.
- [22] Mads M. Pedersen et al. *PyWake 2.5.0: An open-source wind farm simulation tool*. DTU Wind, Technical University of Denmark, <https://gitlab.windenergy.dtu.dk/TOPFARM/PyWake>.
- [23] N.O. Jensen. *A note on wind generator interaction*. Risø-M 2411. Risø National Laboratory, 1983.
- [24] I. Katic, J. Højstrup, and N.O. Jensen. “A Simple Model for Cluster Efficiency.” In: *EWEC’86. Proceedings. Vol. 1*. 1987, pp. 407–410.
- [25] R. J. Barthelmie et al. “Comparison of Wake Model Simulations with Offshore Wind Turbine Wake Profiles Measured by Sodar.” In: *Journal of Atmospheric and Oceanic Technology* 23.7 (2006), pp. 888–901.
- [26] National Renewable Energy Laboratory. *FLORIS: Flow Redirection and Induction in Steady State*. <https://github.com/nrel/floris>. Accessed: 2024-02-15.
- [27] Riccardo Riva et al. *Welcome to TOPFARM*. <https://topfarm.pages.windenergy.dtu.dk/TopFarm2/index.html>. Accessed: 2023-09-25.
- [28] ABB. *XLPE Submarine Cable Systems. Attachment to XLPE Land Cable systems - User’s Guide*. 2010. URL: <https://new.abb.com/docs/default-source/ewea-doc/xlpe-submarine-cable-systems-2gm5007.pdf>.
- [29] DTU Wind and Energy Systems. *TOPFARM / EDWIN · GitLab*. <https://gitlab.windenergy.dtu.dk/TOPFARM/edwin/tree/dev>. Accessed: 2024-01-26.
- [30] John Forrest et al. *Coin-or/Cbc: Release Releases/2.10.11*. <https://zenodo.org/records/10041724>. Accessed: 2024-01-26.
- [31] DTU Wind and Energy Systems. *Collection System Layout for IEA Wind 740-10-MW Reference OWPP*. [https://gitlab.windenergy.dtu.dk/TOPFARM/edwin/tree/dev/docs/notebooks/IEA37\\_Borssele\\_Cable\\_Optimization.ipynb](https://gitlab.windenergy.dtu.dk/TOPFARM/edwin/tree/dev/docs/notebooks/IEA37_Borssele_Cable_Optimization.ipynb). Accessed: 2024-02-06.

## A Regular Layout

Table 5: Turbine coordinates and cable connections for the regular grid layout. Coordinates refer to the EPSG:25831 coordinate reference system. Con. = Connection to Turbine ID or Substation (S); CT = Cable Type according to Table 4.

#	Northing [m]	Easting [m]	Con.	CT	#	Northing [m]	Easting [m]	Con.	CT
1	500,968.2	5,716,452.8	3	1	37	492,983.0	5,728,654.6	49	2
2	499,748.7	5,717,635.9	5	1	38	491,484.5	5,727,853.7	38	2
3	501,245.8	5,718,427.2	7	1	39	490,265.0	5,729,036.7	51	2
4	500,026.3	5,719,610.3	9	1	40	488,766.6	5,728,235.8	30	1
5	498,527.8	5,718,809.4	6	1	41	487,547.1	5,729,418.9	53	1
6	497,308.3	5,719,992.5	11	1	42	502,633.9	5,728,299.4	32	1
7	501,523.4	5,720,401.7	8	1	43	501,414.4	5,729,482.5	45	1
8	500,303.9	5,721,584.7	15	2	44	499,916.0	5,728,681.6	46	2
9	498,805.5	5,720,783.8	10	1	45	498,696.5	5,729,864.6	S	2
10	497,586.0	5,721,966.9	16	1	46	497,198.0	5,729,063.8	S	3
11	496,087.5	5,721,166.0	17	2	47	495,978.5	5,730,246.8	S	3
12	494,868.0	5,722,349.1	19	1	48	494,480.1	5,729,445.9	48	3
13	501,801.0	5,722,376.1	14	1	49	493,260.6	5,730,629.0	S	3
14	500,581.5	5,723,559.2	21	1	50	491,762.1	5,729,828.1	50	3
15	499,083.1	5,722,758.3	23	2	51	490,542.6	5,731,011.2	61	2
16	497,863.6	5,723,941.3	25	2	52	489,044.2	5,730,210.3	40	2
17	496,365.1	5,723,140.4	18	2	53	487,824.7	5,731,393.3	63	1
18	495,145.7	5,724,323.5	26	3	54	486,326.2	5,730,592.5	42	1
19	493,647.2	5,723,522.6	20	1	55	485,106.8	5,731,775.5	55	1
20	492,427.7	5,724,705.7	27	1	56	497,475.7	5,731,038.2	S	3
21	502,078.7	5,724,350.5	22	1	57	496,256.2	5,732,221.3	S	3
22	500,859.2	5,725,533.6	33	2	58	494,757.7	5,731,420.4	S	3
23	499,360.7	5,724,732.7	24	3	59	493,538.2	5,732,603.4	59	3
24	498,141.2	5,725,915.8	S	3	60	492,039.8	5,731,802.5	60	2
25	496,642.8	5,725,114.9	35	2	61	490,820.3	5,732,985.6	70	1
26	495,423.3	5,726,297.9	S	3	62	489,321.8	5,732,184.7	52	1
27	493,924.8	5,725,497.1	28	2	63	488,102.3	5,733,367.8	71	1
28	492,705.3	5,726,680.1	37	2	64	486,603.9	5,732,566.9	54	1
29	491,206.9	5,725,879.2	30	1	65	497,753.3	5,733,012.6	57	2
30	489,987.4	5,727,062.3	39	1	66	496,533.8	5,734,195.7	66	2
31	502,356.3	5,726,325.0	22	1	67	495,035.3	5,733,394.8	58	3
32	501,136.8	5,727,508.0	45	1	68	493,815.9	5,734,577.9	68	2
33	499,638.3	5,726,707.1	34	3	69	492,317.4	5,733,777.0	69	2
34	498,418.9	5,727,890.2	S	3	70	489,599.4	5,734,159.1	62	1
35	496,920.4	5,727,089.3	47	3	71	498,030.9	5,734,987.1	67	1
36	495,700.9	5,728,272.4	S	3	72	496,811.4	5,736,170.1	72	1
37	494,202.5	5,727,471.5	36	3	73	495,313.0	5,735,369.2	67	1

## B Irregular Layout

Table 6: Turbine coordinates and cable connections for the irregular layout. Coordinates refer to the EPSG:25831 coordinate reference system. Con. = Connection to Turbine ID or Substation (S); CT = Cable Type according to Table 4.

#	Northing [m]	Easting [m]	Con.	CT	#	Northing [m]	Easting [m]	Con.	CT
1	501,266.5	5,715,995.9	51	1	38	497,223.8	5,723,028.6	52	2
2	493,922.3	5,723,126.8	35	1	39	497,332.0	5,736,641.5	28	1
3	502,907.2	5,727,400.0	9	2	40	496,443.6	5,729,036.2	S	3
4	502,095.1	5,721,783.9	13	2	41	499,696.1	5,730,763.2	56	1
5	496,804.7	5,720,326.9	21	1	42	497,791.5	5,727,794.8	S	3
6	485,102.8	5,731,616.7	33	1	43	503,157.7	5,729,153.3	26	3
7	490,588.4	5,726,359.0	36	1	44	502,656.9	5,725,664.9	8	1
8	502,784.8	5,726,554.8	3	1	45	499,014.0	5,718,720.2	23	2
9	503,032.6	5,728,282.6	43	2	46	502,389.7	5,723,814.4	34	3
10	484,578.2	5,732,113.1	6	1	47	499,568.7	5,717,641.9	45	1
11	486,707.1	5,733,272.0	25	1	48	498,412.3	5,736,984.3	66	1
12	492,087.7	5,734,978.8	19	1	49	500,126.6	5,737,528.6	66	1
13	502,245.1	5,722,819.6	46	2	50	493,699.5	5,728,053.3	S	3
14	486,993.7	5,729,811.2	27	1	51	500,599.4	5,716,646.9	47	1
15	486,339.9	5,730,437.8	14	1	52	497,855.6	5,725,266.3	42	3
16	501,937.2	5,720,684.8	4	1	53	495,278.3	5,735,992.4	60	1
17	490,866.2	5,734,594.0	30	2	54	493,700.9	5,731,256.9	29	3
18	489,584.0	5,734,183.8	17	1	55	492,224.4	5,729,156.7	S	3
19	493,245.0	5,735,342.2	60	1	56	498,554.4	5,731,292.3	S	2
20	484,184.9	5,732,482.2	10	1	57	489,085.3	5,727,820.4	31	2
21	495,837.3	5,721,263.8	38	2	58	500,588.5	5,730,350.5	41	1
22	501,763.7	5,719,469.0	16	1	59	499,488.7	5,736,258.4	62	2
23	497,805.7	5,719,362.4	68	2	60	494,285.3	5,735,679.6	61	3
24	502,520.0	5,724,758.0	44	1	61	495,302.2	5,733,057.1	S	3
25	488,197.0	5,733,753.4	18	1	62	498,899.6	5,735,074.1	65	2
26	502,261.7	5,729,567.1	S	3	63	493,038.7	5,723,984.1	70	2
27	487,660.6	5,729,175.8	32	1	64	494,794.7	5,726,569.8	40	3
28	496,327.0	5,736,318.3	53	1	65	498,335.3	5,733,940.2	72	3
29	495,560.7	5,730,365.5	S	3	66	499,450.5	5,737,313.6	59	1
30	492,442.8	5,732,709.5	54	2	67	501,551.8	5,718,018.1	22	1
31	489,811.5	5,727,115.2	50	3	68	499,153.2	5,721,395.3	71	3
32	488,384.8	5,728,488.3	57	2	69	489,444.0	5,731,966.5	74	2
33	485,719.3	5,731,024.7	69	2	70	495,667.2	5,725,151.8	64	2
34	499,693.2	5,726,888.9	S	3	71	499,425.1	5,723,990.6	S	3
35	494,872.6	5,722,212.0	21	1	72	497,613.7	5,732,484.2	S	3
36	491,373.5	5,725,600.7	37	1	73	501,417.3	5,729,964.4	58	1
37	492,179.3	5,724,816.0	63	1	74	490,809.4	5,730,587.0	55	3